

Barrier-free intermolecular proton transfer induced by excess electron attachment to the complex of alanine with uracil

Iwona Dąbkowska and Janusz Rak

Department of Chemistry, University of Gdańsk, Sobieskiego 18, 80-952 Gdańsk, Poland

Maciej Gutowski^{a)}

Department of Chemistry, University of Gdańsk, Sobieskiego 18, 80-952 Gdańsk, Poland

and Chemical Sciences Division, Pacific Northwest National Laboratory, Richland, Washington 99352

J. Michael Nilles, Sarah T. Stokes, and Kit H. Bowen, Jr.

Department of Chemistry, Johns Hopkins University, Baltimore, Maryland 21218

(Received 24 February 2003; accepted 14 January 2004)

The photoelectron spectrum of the uracil–alanine anionic complex (UA)[−] has been recorded with 2.540 eV photons. This spectrum reveals a broad feature with a maximum between 1.6 and 2.1 eV. The vertical electron detachment energy is too large to be attributed to an (UA)[−] anionic complex in which an intact uracil anion is solvated by alanine, or vice versa. The neutral and anionic complexes of uracil and alanine were studied at the B3LYP and second-order Møller–Plesset level of theory with 6-31++G** basis sets. The neutral complexes form cyclic hydrogen bonds and the three most stable neutral complexes are bound by 0.72, 0.61, and 0.57 eV. The electron hole in complexes of uracil with alanine is localized on uracil, but the formation of a complex with alanine strongly modulates the vertical ionization energy of uracil. The theoretical results indicate that the excess electron in (UA)[−] occupies a π^* orbital localized on uracil. The excess electron attachment to the complex can induce a barrier-free proton transfer (BFPT) from the carboxylic group of alanine to the O8 atom of uracil. As a result, the four most stable structures of the uracil–alanine anionic complex can be characterized as a neutral radical of hydrogenated uracil solvated by a deprotonated alanine. Our current results for the anionic complex of uracil with alanine are similar to our previous results for the anion of uracil with glycine [*Eur. Phys. J. D* **20**, 431 (2002)], and together they indicate that the BFPT process is not very sensitive to the nature of the amino acid's hydrophobic residual group. The BFPT to the O8 atom of uracil may be relevant to the damage suffered by nucleic acid bases due to exposure to low energy electrons. © 2004 American Institute of Physics. [DOI: 10.1063/1.1666042]

I. INTRODUCTION

Low-energy electrons and electron holes are produced through interaction of radiation with the living cell environment. Low-energy electrons appear as a secondary product of radiolysis of water, with the primary products being the HO and H radicals.¹ Until now, the genotoxicity of radiation was primarily studied in the context of these radicals, and the connection between their presence and mutations of DNA is well documented.^{2,3} Only in the last decade has it become clear that direct interactions with charged particles in a radiation field account for a significant fraction of the radiation damage to DNA in cells.⁴ This reversal in traditional focus derives primarily from a reassessment of the radical-scavenging capacity of the intracellular medium, i.e., OH damage to DNA is limited to those radicals which were formed within a few nanometers of the DNA. Current estimates place direct damage at about one-third of the total.⁴

The recent experiments of Sanche and co-workers suggest that electrons with energies in a range 1–20 eV can induce DNA damage.^{1,5} The authors suggested that excess

electrons trapped in temporary anionic states initiate chemical reactions leading to single- and double-strand breaks. Such a mechanism of a single-strand break has been computationally studied by Barrios *et al.*, who suggested that only a small barrier would have to be overcome to create a sugar-phosphate C–O bond rupture initiated by an excess electron attachment to a DNA base.⁶

Negatively charged clusters of biologically important molecules have been extensively studied, both experimentally^{7–9} and theoretically.^{10–15} Electron trapping on nucleic acid bases has been an important topic in radiation biology for several decades. Then, ten years ago, it was realized that the large polarity of these molecules allows for the existence of dipole-bound anionic states as well.¹⁰ While our recent coupled cluster single double (triple) [CCSD(T)] results indicate that the valence anionic state of uracil (U) is vertically stable with respect to the neutral by 0.507 eV,¹⁶ our calculations also find the valence anionic state to be thermodynamically unstable by 0.215 eV with respect to the dipole-bound anionic state and by 0.147 eV with respect to the neutral. The current view is that valence anionic states are unbound, or at best very weakly bound, for isolated nucleic acid bases, but become dominant for solvated species.^{15,17}

^{a)}Electronic mail: maciej.gutowski@pnl.gov

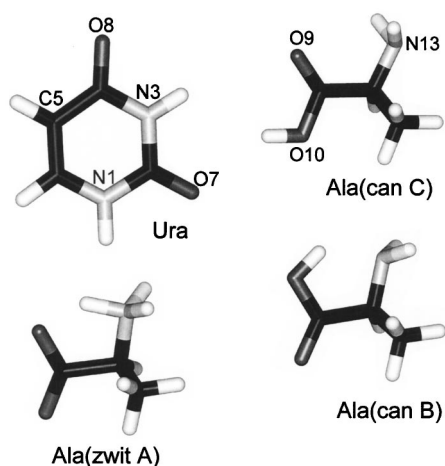
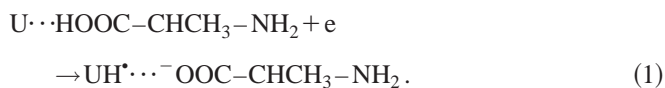


FIG. 1. The lowest energy tautomers and conformers of alanine and uracil.

The intra- and intermolecular tautomerizations involving nucleic acid bases have long been suggested as critical steps in mutations of DNA.^{18,19} Intramolecular proton transfer reactions have been studied for both isolated and hydrated nucleic acid bases.⁷ Intermolecular single and double proton transfer reactions have been studied for the dimers of nucleic acid bases in both their ground and excited electronic states.²⁰ Only small activation barriers were found for the anionic and cationic GC pair, with the proton transfer reaction being favorable for the anion and slightly unfavorable for the cation.²⁰

Recently we described a tautomerization process, which is induced by the attachment of an excess electron to the complex of uracil with glycine.¹⁶ The electron attachment leads to a barrier-free proton transfer (BFPT) from the carboxylic group of glycine to the O8 atom of uracil with the products being a neutral radical of hydrogenated uracil (UH^\bullet) and an anion of deprotonated glycine (see Fig. 1 for the numbering of atoms of uracil). An important question arises as to whether amino acids with a residual group more complex than the H of glycine have a similar propensity to the barrier-free proton transfer. Hence, in the present study we investigate the anionic uracil–alanine (UA^-) complex. Interactions between uracil and alanine have recently been studied in the context of molecular recognition process.²¹

Results of our photoelectron spectroscopic experiments and quantum chemical calculations reported in the current study strongly suggest that alanine acts in a similar way as does glycine in its anionic complexes with uracil. Our calculations predict that a BFPT occurs from the carboxylic group of alanine (A) to the O8 atom of uracil:



Thus, our current results indicate that the BFPT process is not very sensitive to the nature of the amino acid's hydrophobic residual group. In the future we will explore how amino acids with hydrophilic residual groups, such as aspartic or glutamic acids, interact with nucleic acid bases upon an excess electron attachment.

An interesting point here is that attachment of low-energy electrons to complexes of RNA or DNA with proteins may also lead to mutations. The uracil–alanine complex is a model system only, but our results demonstrate the possibility of electron-induced mutations in DNA–protein complexes, e.g., during transcription. The formation of neutral radicals of hydrogenated pyrimidine nucleic acid bases could play an important role in damage to DNA and RNA by low energy electrons. For instance, thymine hydrogenated at the O8 position cannot form a hydrogen bond with adenine, as dictated by the Watson–Crick pairing scheme. Such a UH^\bullet (thymine– H^\bullet) radical might also react with an adjacent ribose (deoxyribose) molecule triggering strand-breaks in nucleic acids.

Analysis of anionic states in complexes of uracil with alanine requires basic understanding of neutral complexes, which are governed by hydrogen bonding. Hence, our description of anionic states is preceded by the analysis of neutral complexes. Their stability provides a reference point for the stability of anionic structures and their polarity allows us to judge how important dipole-bound anionic states might be in these complexes. Finally, the effect of complex formation on the vertical ionization energy of uracil is discussed.

II. METHODS

A. Experiment

Negative ion photoelectron spectroscopy is conducted by crossing a mass-selected beam of negative ions with a fixed-frequency laser beam and energy-analyzing the resultant photodetached electrons.²² It is governed by the energy-conserving relationship: $h\nu = \text{EBE} + \text{EKE}$, where $h\nu$ is the photon energy, EBE is the electron binding energy, and EKE is the electron kinetic energy. One knows the photon energy of the experiment, one measures the electron kinetic energy spectrum, and then by difference, one obtains electron binding energies, which in effect are the transition energies from the anion to the various energetically accessible states of its corresponding neutral.

Our apparatus has been described elsewhere.²³ To prepare the species of interest, a mixture of uracil and alanine was placed in the stagnation chamber of a nozzle source and heated to $\sim 180^\circ\text{C}$. Argon gas at a pressure of 1–2 atm was used as the expansion gas, and the nozzle diameter was 25 μm . Electrons were injected into the emerging jet expansion from a biased Th/Ir filament in the presence of an axial magnetic field. The resulting anions were extracted and mass-selected with a magnetic sector mass spectrometer. Electrons were then photodetached from the selected anions with ~ 100 circulating watts of 2.540 eV photons and finally energy-analyzed with a hemispherical electron energy analyzer.

B. Computation

As this computational effort is a continuation of our previous studies on the neutral²⁴ and anionic¹⁶ complexes of uracil and glycine, we will use analogous notation for hydrogen-bonded structures and the same computational methodology. The anionic structures characterized in the cur-

rent study will be labeled as aUAN, indicating the *parent* neutral structure UAN the anionic structure is related to. More precisely, an anionic structure aUAN is determined in the course of geometry optimization initialized from the optimal geometry for the neutral structure UAN. The structures UAN for the neutral uracil–alanine complexes are analogous to the uracil–glycine UGN structures characterized in Ref. 24. The L and D enantiomers of alanine must have identical chemical properties toward uracil, and thus, only the L enantiomer is considered here.

The stability of the neutral (superscript=0) or anionic (superscript=−) UA complexes is expressed in terms of E_{stab} , H_{stab} , and G_{stab} . E_{stab} is defined as a difference in electronic energies of the monomers and the dimer

$$E_{\text{stab}} = E^{\text{UA}(0,-)}(\text{Geom}^{\text{UA}(0,-)}) - E^{\text{U}(0,-)}(\text{Geom}^{\text{U}(0,-)}) - E^{\text{A}}(\text{Geom}^{\text{A}}) \quad (2)$$

with the electronic energy E^{X} ($\text{X} = \text{U}^{(0,-)}, \text{A}, \text{UA}^{(0,-)}$) computed for the coordinates determining the optimal geometry of X (i.e., the geometry where E^{X} is at the minimum). The values of E_{stab} were not corrected for basis set superposition errors because our earlier results demonstrated that the values of this error in B3LYP/6-31++G** calculations for a similar neutral uracil–glycine complex did not exceed 0.06 eV.²⁴ The stabilization enthalpy H_{stab} results from correcting E_{stab} for zero-point vibration terms, thermal contributions to energy from vibrations, rotations, and translations, and the pV terms. Finally, the stabilization Gibbs energy G_{stab} results from supplementing H_{stab} with the entropy term. The values of H_{stab} and G_{stab} discussed in the following were obtained for $T = 298$ K and $p = 1$ atm in the harmonic oscillator-rigid rotor approximation.

As our primary research method we applied density functional theory (DFT) with a Becke's three parameter hybrid functional (B3LYP)^{25–27} and a modified Perdew–Wang one-parameter-method for kinetics (MPW1K) designed by Truhlar *et al.*²⁸ In both DFT approaches we used the same 6-31++G** basis set.^{29,30} Five d functions were used on heavy atoms. The usefulness of the B3LYP/6-31++G** method to describe intra- and intermolecular hydrogen bonds has been demonstrated in recent studies through comparison with the second-order Møller–Plesset predictions.^{24,31} The ability of the B3LYP method to predict excess electron binding energies has recently been reviewed and the results were found to be satisfactory for valence-type molecular anions.³² We found that the value of electron vertical detachment energy (VDE) determined at the B3LYP/6-31++G** level for the valence π^* anionic state of an isolated uracil is overestimated by 0.2 eV in comparison with the CCSD(T)/aug-cc-pVDZ result.¹⁶ We will assume in the following that the same correction of 0.2 eV applies to the values of VDE for all anionic UA complexes in which an excess electron occupies a π^* orbital localized on uracil.

It is known that the B3LYP method underestimates barriers for proton transfer reactions,²⁸ and thus, the lack of a barrier for the proton transfer reaction (1) may be an artifact of the B3LYP method. For this reason, we performed additional geometry optimizations using the MPW1K exchange–

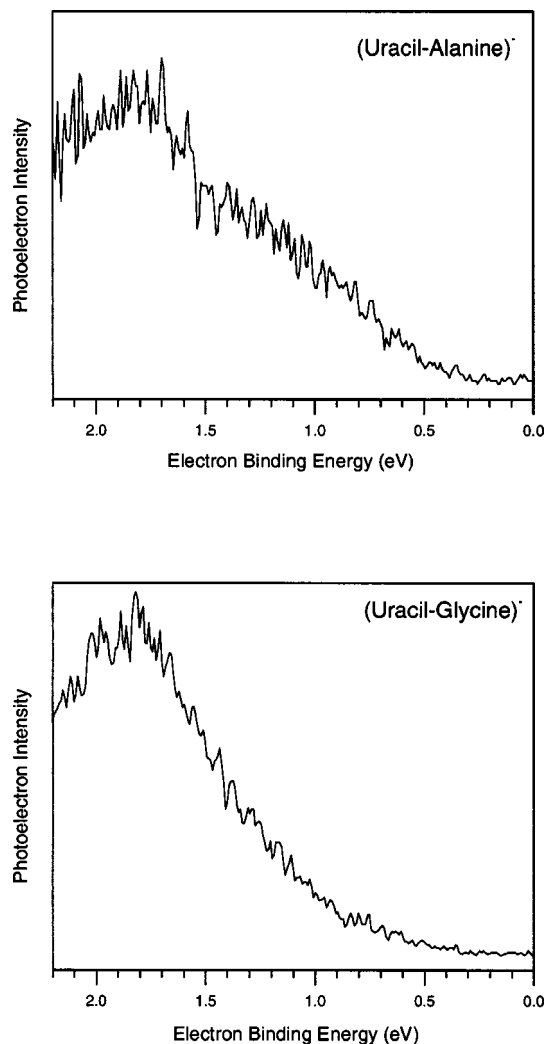


FIG. 2. Photoelectron spectra of (a) uracil–alanine dimer anion and (b) uracil–glycine dimer anion, both recorded with 2.540 eV/photon.

correlation functional, which was parametrized to reproduce barrier heights for chemical reactions.²⁸ Finally, MP2 geometry optimizations have been performed for three anionic UA complexes to provide more insight into the reaction path connecting the $\text{U}^- \cdots \text{HOOC}-\text{CHCH}_3-\text{NH}_2$ and $\text{UH}^* \cdots ^-\text{OOC}-\text{CHCH}_3-\text{NH}_2$ structures. The qualitative agreement between the MP2, B3LYP, and MPW1K predictions strengthens our conclusion.

All calculations were carried out with the GAUSSIAN 98³³ and NWCHEM³⁴ codes on a cluster of 32 bit Xeon/SCI Dolphin processors, DEC Alpha 533au two-processor workstation, IBM SP/2, and SGI 2800 and Origin2000 numerical servers.

III. RESULTS

A. Photoelectron spectra

The photoelectron spectra for the uracil–alanine and uracil–glycine anionic complexes are quite similar. Both are presented in Fig. 2. Each spectrum exhibits a broad, structureless feature. For (UG)[−], its maximum occurs at EBE = 1.8 eV, while for (UA)[−], its maximum occurs between

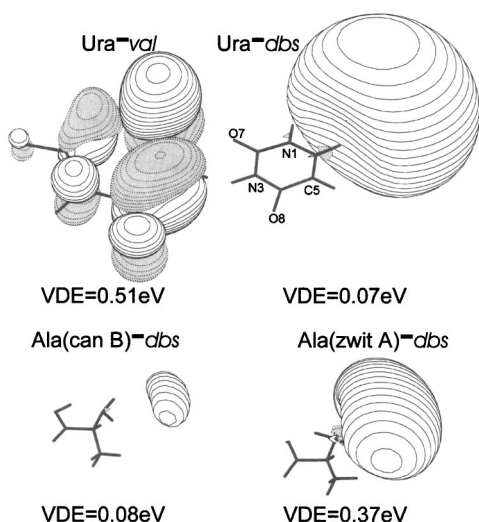


FIG. 3. The excess electron orbital for the valence π^* and dipole-bound states of uracil (top) and in dipole-bound anionic states of canonical and zwitterionic alanine (bottom). We have applied a contour line spacing of $0.03 \text{ bohr}^{-3/2}$ for the valence anion and $0.021 \text{ bohr}^{-3/2}$ for dipole-bound states of alanine and $0.008 \text{ bohr}^{-3/2}$ for the dipole-bound state of uracil.

EBE=1.6–2.1 eV. The photoelectron spectrum of UA^- cannot be attributed to an intact U^- solvated by alanine. As mentioned earlier, the valence π^* and dipole-bound anionic states of uracil are characterized by a calculated value of VDE of 0.507 and 0.073 eV, respectively¹⁶ (see Fig. 3 for the excess electron charge distributions in these systems). Henceforth, only the valence π^* anionic state will be considered further, since the experimental value of VDE for UA^- is far too large for the dipole-bound anionic state of U solvated by A. However, the experimental value of VDE is also too large for the valence π^* anionic state of U solvated by A. The solvation energy by alanine would have to be larger by ~ 1.3 eV, for the anion over its corresponding neutral, in order to be consistent with the maximum in the photoelectron spectrum. This is rather improbable given that the VDE of $\text{U}^-(\text{H}_2\text{O})_1$ is only 0.9 eV.³⁵

Similarly, attributing the broad peak for $(\text{UA})^-$ to an anion of intact alanine solvated by uracil is inappropriate. The reason is that the most stable conformer of canonical alanine, labeled “can C” in Fig. 1, does not bind an electron³⁶ and the measured electron affinity (EA) of alanine is ~ -1.8 eV.³⁷ Our theoretical results indicate that alanine forms only weakly bound anions with VDE values, determined at the MP2 level, of 0.08 and 0.37 eV for the canonical (can B) and zwitterionic (zwit A) structure, respectively³⁶ (see Fig. 1 for the tautomers and conformers of alanine and Fig. 3 for the excess electron charge distributions in these systems). The electron binding energy shift induced by the interaction with uracil would have to be approximately 1.4 eV to be consistent with the maximum of the photoelectron peak for $(\text{UA})^-$, which is rather improbable.

Uracil in anionic complexes with alanine behaves much like uracil in anionic complexes with glycine (see Fig. 2). We expect that BFPT occurs in anionic complexes of alanine with uracil, in analogy to the anionic uracil–glycine complexes.¹⁶ However, there is also a difference in the pho-

toelectron spectrum of $(\text{UA})^-$ relative to that of $(\text{UG})^-$. When compared to the spectrum of $(\text{UG})^-$, the photoelectron spectrum of $(\text{UA})^-$ appears to have additional intensity in the EBE region between 0.5 and 1.4 eV. This may indicate a significant presence of non-BFPT anionic complexes among the $(\text{UA})^-$ species, as compared to the $(\text{UG})^-$ species, although the most stable anionic conformers underwent BFPT in the anionic complexes of U with both amino acids.

Lastly, the widths of the main spectral features for UA^- and UG^- are much greater than of the photoelectron features for the valence anionic state of uracil solvated by either a single water molecule or a xenon atom.³⁵ While this is mainly additional evidence that these complexes are not valence uracil anions solvated by neutrals, it may also indicate that several anionic conformers of the uracil–amino acid complexes coexist, especially in the case of $(\text{UA})^-$, in the gas phase under our experimental conditions.

B. Computational results

1. Neutral uracil–alanine complexes

Alanine and glycine have analogous proton donor and acceptor sites, which are suitable for forming hydrogen bonds with uracil. The replacement of a hydrogen atom by a methyl group in alanine can create at most steric obstacles that have to be negotiated upon formation of hydrogen bonds. Hence, the topological space for the neutral UA complex is at least as complicated as was observed for the neutral UG complex. For the latter, we characterized 23 hydrogen-bonded structures formed by the lowest energy tautomers of U and G.²⁴ In the current study only a limited subset of these 23 structures was explored. First, we present the uracil–alanine structures, labeled UA1–UA4, which are analogous to the four most stable structures of UG. Second, we will study additional structures, labeled UAN ($n = 14, 16, 18, 20$), which are analogous to the UGn structures with the same numerals.²⁴ The structures from the latter UGn set were not remarkably stable for neutral complexes but they led to relatively stable anionic structures.¹⁶

The neutral UAN complexes are displayed in Fig. 4 and their B3LYP/6-31++G^{**} characteristics are given in Table I. These are cyclic structures with two hydrogen bonds. The most stable complexes are UA1–UA4 with the carbonyl (O9) and hydroxyl (O10H) groups of alanine interacting with the proton donor and acceptor centers of uracil. The UA1, UA2, and UA3 structures have two strong hydrogen bonds and the values of E_{stab} span a range of -0.72 to -0.57 eV. The values of G_{stab} are negative for these three structures indicating a thermodynamic preference to form the uracil–alanine dimer. The UA4 structure, with one weak $\text{C5H}\cdots\text{O9}$ hydrogen bond, is stable by only -0.45 eV in terms of E_{stab} and unstable in terms of G_{stab} , as are other UAN structures ($n = 14, 16, 18, 20$). The diminished stability of UA14 and UA16 results from the fact that the O10H hydroxyl group acts as a proton donor and acceptor. The small stability of UA18 and UA20 results from a geometrical mismatch between the proton donor and acceptor sites of interacting monomers.²⁴

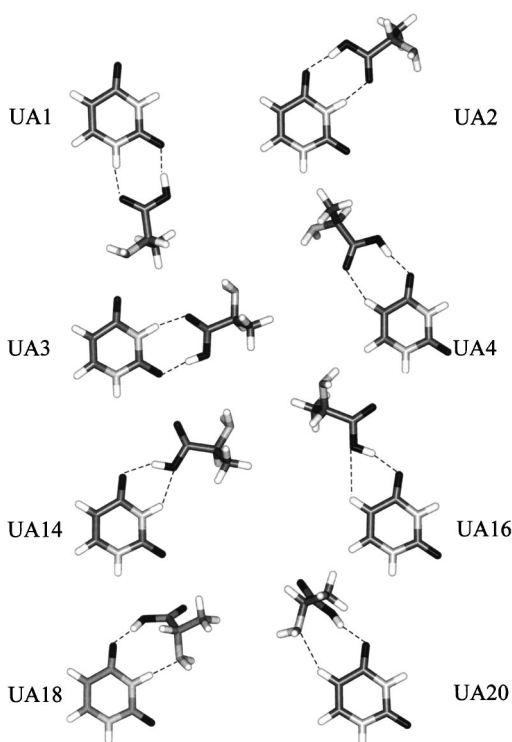


FIG. 4. Optimized structures of neutral complexes of alanine with uracil.

The dipole moments of uracil and alanine provide insight into whether anionic dipole-bound states of UA_n complexes can contribute to the photoelectron spectrum reported in Fig. 2. The dipole moment for the most stable conformer of canonical alanine (can C) is smaller than the critical dipole moment of $\sim 2.5 D^7$ required for excess electron binding, but a less stable conformer, can B, is characterized by a larger dipole moment of 5.9 D. The calculated dipole moments of the UA_n complexes do not exceed 8.2 D. These dipole moments are too small to support a dipole-bound anionic state with a VDE of ~ 1.8 eV.

The vertical ionization potentials (VIP) for alanine, uracil, and the UA_n complex are given in Table I. The calculated VIP of alanine of 9.6 eV is in good agreement with

TABLE I. Uracil–alanine neutral complexes' B3LYP/6-31++G** characteristics. Energies in eV, dipole moments μ in D. E_{stab} and G_{stab} stand for the energy and Gibbs free energy of stabilization, respectively [see Eq. (2)]. ZPVE is a correction from zero-point vibrations, VIP is the vertical ionization potential, and $S \rightarrow T$ is the singlet–triplet splitting at the optimal geometry of the singlet state.

Structure	E_{stab}	$E_{\text{stab}} + \text{ZPVE}$	G_{stab}	μ	VIP	$S \rightarrow T$
UA1	-0.72	-0.67	-0.18	2.91	8.86	3.62
UA2	-0.61	-0.57	-0.08	5.76	8.74	3.59
UA3	-0.57	-0.52	-0.04	6.05	8.77	3.65
UA4	-0.47	-0.42	0.02	4.02	8.74	3.56
UA14	-0.33	-0.30	0.12	7.20	8.75	3.59
UA16	-0.31	-0.28	0.10	6.84	8.70	3.59
UA18	-0.38	-0.32	0.18	7.69	9.05	3.60
UA20	-0.10	-0.06	0.38	8.17	8.95	3.57
Ala can C				1.35	9.61	5.13
Ala can B				5.89	9.86	5.17
Ura				4.66	9.46	3.60

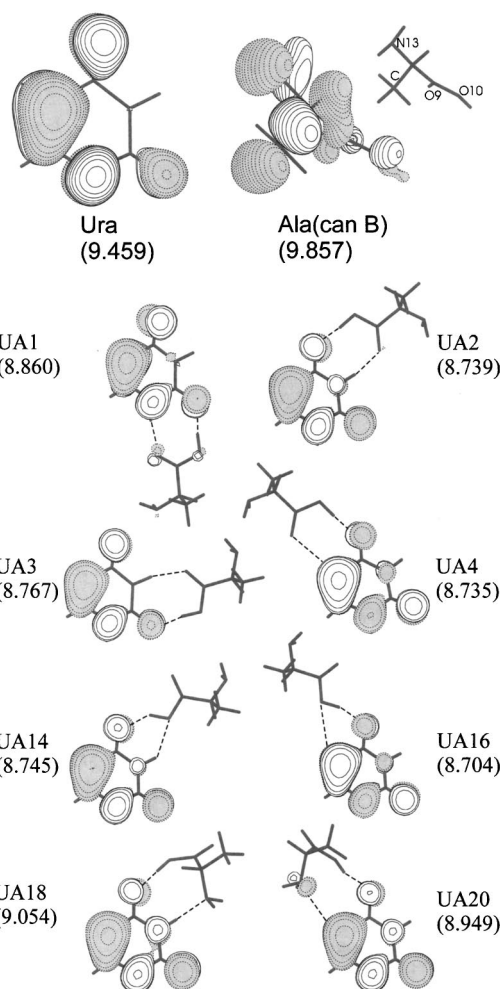


FIG. 5. The orbital that describes electron hole in isolated uracil and canonical alanine (a) and in the UA_n complexes. The singly occupied orbitals for the cations were plotted with a contour line spacing of $0.03 \text{ bohr}^{-3/2}$. The B3LYP/6-31++G** values of vertical ionization potentials are in parentheses (eV).

the experimental result of 9.8 eV reported by Debies *et al.*³⁸ The calculated VIP for uracil is smaller by 0.1 eV than for alanine, and the agreement with the experimental result of 9.59 eV is also satisfactory.³⁹ In uracil, the electron hole is localized primarily on the C5–C6 bond, whereas in alanine it is delocalized throughout the whole molecule [see Fig. 5(a)]. The electron hole is localized on uracil in the UA_n complexes [see Fig. 5(b)] and its distribution is strikingly similar to the distribution in isolated uracil. The bonding with alanine lowers, however, the value of VIP for every UA_n complex considered here, and the largest shift by 0.8 eV is observed for $n = 16, 4, 2$, and 14. Formation of a complex with alanine strongly modulates the vertical ionization energy of uracil.

2. Anionic uracil–alanine complexes

The results of B3LYP/6-31++G** calculations for anions of various hydrogen-bonded uracil–alanine complexes are summarized in Table II and representative structures are displayed in Fig. 6. A common feature of anionic wave functions identified by us for the UA complexes is that the excess

TABLE II. Uracil–alanine anionic complexes' B3LYP/6-31++G** characteristics. Energies in eV. E_{stab} and G_{stab} stand for the energy and Gibbs free energy of stabilization, respectively [see Eq. (2)]. ZPVE is a correction from zero-point vibrations, VDE is the electron vertical detachment energy, EA is electron affinity, and $S \rightarrow T$ is the singlet–triplet splitting for the neutral complex at the optimal geometry of the doublet anion. Qualitative information (Yes/No) is provided whether an anionic structure undergoes BFPT.

Structure	E_{stab}	$E_{\text{stab}} +$		VDE	EA	$S \rightarrow T$	BFPT	
		ZPVE	G_{stab}				B3LYP	MPW1K
aUA1	-0.94	-0.95	-0.47	1.09	0.31	2.80	No	No
aUA2	-1.21	-1.21	-0.75	1.90	0.68	2.60	Yes	Yes
aUA3	-0.80	-0.78	-0.32	1.11	0.31	2.70	No	No
aUA4	-1.09	-1.11	-0.67	2.03	0.71	2.51	Yes	Yes
aUA14	-1.11	-1.10	-0.65	2.20	0.86	2.42	Yes	Yes
aUA16	-1.06	-1.08	-0.67	2.18	0.83	2.43	Yes	Yes
aUA18	-0.92	-0.93	-0.42	1.98	0.63	2.55	Yes	No
aUA20	-1.00	-1.01	-0.60	1.72	0.98	2.79	No	No

electron is localized on a π^* orbital of uracil, in close resemblance to the valence anionic state of isolated uracil (see Figs. 3 and 6).¹² A neutral molecule of isolated uracil has a symmetry plane.^{11,24} However, occupation of the antibonding π orbital by an excess electron induces buckling of the ring because nonplanar structures are characterized by a less severe antibonding interaction.^{11,12,16} The same kind of ring distortion takes place in all UA complexes upon an excess electron attachment.

Our most important finding is that the most stable anionic structures are characterized by a BFPT from the carboxylic group of alanine to the O8 atom of uracil, see Table II and Fig. 6. The driving force for the proton transfer is to stabilize the excess negative charge, which is primarily lo-

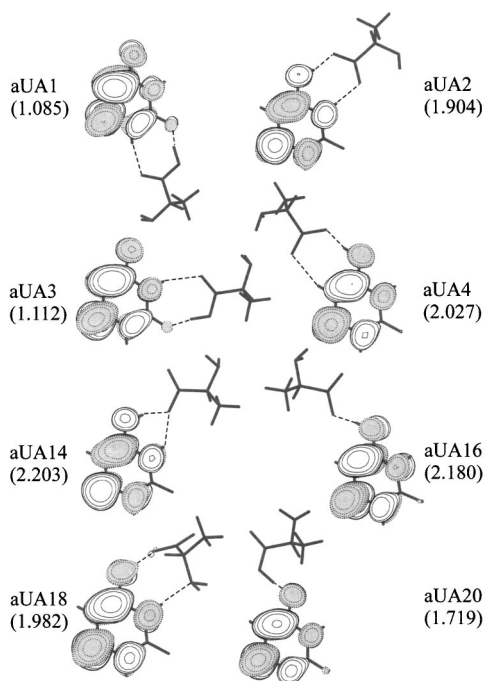
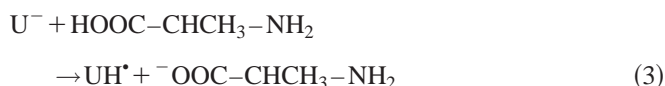


FIG. 6. The structure and excess electron charge distribution in the uracil–alanine complexes. The orbitals were plotted with a contour line spacing of $0.03 \text{ bohr}^{-3/2}$. The B3LYP/6-31++G** values of electron vertical detachment energies are in parentheses (eV).

calized in the O8–C4–C5–C6 region. In consequence of the extra stabilization of the excess electron provided by the transferred proton, the values of VDE for the aUA2, aUA14, aUA4, aUA16, and aUA18 structures are larger by more than 1.4 eV than for the valence anion of an isolated uracil. In fact, the calculated values of VDE for these structures span a range of 2.2–1.9 eV. After correcting downward by 0.2 eV, the resulting range of 2.0–1.7 eV coincides well with the broad peak in the photoelectron spectrum, see Fig. 2.

The products of the intermolecular tautomerization reactions are the neutral radical UH^* , with the O8 atom hydrogenated, and the deprotonated alanine (see Fig. 6). We found that deprotonation of alanine is highly endothermic and requires 15.0 eV. On the other hand, protonation of the valence anion of uracil is exothermic by 14.7 eV. Hence, a hypothetical reaction, which leads to noninteracting products,



is endothermic by 0.3 eV. For the proton transfer to occur, the stabilizing interaction in the $\text{UH}^* \cdots {}^-\text{OOC-CHCH}_3\text{-NH}_2$ system needs to: (i) compensate this barrier, and (ii) provide at least as much of the stabilization between the UH^* and ${}^-\text{OOC-CHCH}_3\text{-NH}_2$ systems as the untransformed U^- and $\text{HOOC-CHCH}_3\text{-NH}_2$ moieties could provide. Indeed, for the structures with BFPT, i.e., aUA_n ($n=2,4,14,16,18$) E_{stab} varies from -1.21 to -0.92 eV, whereas for the structures without BFPT, i.e., aUA_n ($n=1,3,20$), the values of E_{stab} are smaller: $-0.94 \text{ eV} < E_{\text{stab}} < -0.80 \text{ eV}$. This confirms that occurrence of BFPT requires significant values of E_{stab} and that these would compensate the endothermicity of the reaction (3).

The most stable structure of the anionic complex results from an excess electron attaching to UG2. The neutral complex UA2 is less stable than UA1 by 0.1 eV, hence its population is negligible at standard conditions. Upon electron attachment, however, the COOH proton is transferred without a barrier to the O8 atom of uracil and the most stable anionic structure develops with a VDE value of 1.9 eV (1.7 eV after correcting downward), see Table II and Fig. 6. The adiabatic electron affinity, calculated with respect to the UA2 neutral, is much smaller and amounts to only 0.7 eV.

The neutral structures UA4, UA14, and UA16, which in terms of E_{stab} are less stable than UA1 by 0.2, 0.4, and 0.4 eV, respectively, evolve upon excess electron attachment into the second, third, and fourth most stable anionic structure, respectively. They are separated from the most stable anionic structure aUA2 by only 0.1 eV. Their significant stability and calculated VDEs as large as 2.0–2.2 eV (1.8–2.0 after correcting downward), are also related to the occurrence of BFPT, see Table II and Fig. 6. The adiabatic electron affinities, calculated with respect to the parent neutral structures were found to be 0.7–0.9 eV.

It is known, however, that the B3LYP method underestimates barriers for proton transfer reactions,²⁸ and the lack of a barrier for the proton transfer may be an artifact of the B3LYP method. For this reason, we performed additional MPW1K/6-31++G** geometry optimizations for all an-

ionic uracil–alanine complexes considered in this study. The occurrence of BFPT (yes/no in Table II) proved to be consistent for the B3LYP and MPW1K methods. In addition, MP2/6-31++G** geometry optimizations were performed for the aUAN ($n=1, 2, 4, 14$) complexes starting from the geometry of the corresponding neutral complex. Again, for $n=2, 4, 14$ there was no barrier for proton transfer to the O8 atom and a barrier was detected for $n=1$. These results strongly suggest that the BFPT process proposed by us is not an artifact of the computational B3LYP model.

A preference to transfer a proton to the O8 site is much larger than to the O7 atom, see Fig. 6. In fact, we did not identify any BFPT occurring to the O7 atom of uracil. This may be related to the fact that an excess electron on the π^* orbital is not localized in the neighborhood of the O7 atom.¹⁶ The UA1 and UA3 structures, i.e., the most and third most stable structures of the neutral complex, exemplify this point with no BFPT for aUA1 and aUA3 and the calculated values of VDE of only 1.1 eV for both anionic structures (0.9 eV after correcting downward), see Table II and Fig. 6.

There are at least four anionic structures, which differ in terms of G_{stab} by less than 0.15 eV from the most stable structure aUA2. Three of these structures, aUAN ($n=4, 14, 16$) occur with BFPT and are characterized by large values of VDE. The fourth structure, aUA20, occurs without BFPT and is characterized by a medium value of VDE. They all might contribute to the unusual width of the main feature in the photoelectron spectrum presented in Fig. 2.

It is intriguing which transitions contribute to the PES spectrum with electron binding energies larger than 2.0 eV. The B3LYP/6-31++G** values of the singlet–triplet energy splitting ($S \rightarrow T$) for the neutral UAN complexes are larger than 3 and 2 eV for the optimal neutral and anionic structures, respectively (see Tables I and II). Hence, a significant intensity of the photoelectron spectrum at 2.0 eV has to be related to photodetachment from a doublet state of the anion to the singlet state of the neutral. Transitions to the lowest triplet state of the neutral would require photons with energies above 3 eV.

IV. SUMMARY

The photoelectron spectrum of the uracil–alanine anionic complex was recorded with 2.540 eV photons. This spectrum reveals a broad feature with its maximum between EBE=1.6 and 2.1 eV. The vertical electron detachment energy values are too large to be attributed to the anionic complex of an anion of intact uracil solvated by alanine, or vice versa. The neutral and anionic dimer complexes of uracil and alanine were studied at the density functional level of theory with the B3LYP and MPW1K exchange–correlation functionals and 6-31++G** basis sets to provide interpretation of the photoelectron spectrum. Critical anionic structures were also examined at the MP2/6-31G** level of theory.

For neutral complexes, the largest stabilization energy of 0.72 eV was determined for a structure which involves the N1H and O7 centers of uracil coordinated to the carboxylic group of alanine. The N1 atom, however, is covalently bonded in RNA to the sugar–phosphate backbone. Two other structures, which involve the N3H and either the O8 or O7

sites of uracil, are bound by 0.61 and 0.57 eV, respectively. Dipole moments of the neutral complexes are too small to support dipole-bound anionic states with electron vertical detachment energies in the 1.6–2.1 eV range. The electron hole in complexes of uracil with alanine is localized on uracil but formation of a complex with alanine strongly modulates the vertical ionization energy.

The results of density functional and second-order Møller–Plesset calculations indicate that the excess electron in the uracil–alanine complexes is described by a π^* orbital localized on the ring of uracil. An excess electron on the antibonding π^* orbital induces buckling of the ring. As was previously observed for uracil–glycine complexes,¹⁶ the excess electron can induce a barrier-free proton transfer from the carboxylic group of alanine to the O8 atom of uracil. The driving force for the proton transfer is to stabilize the negative excess charge localized primarily on the O8–C4–C5–C6 fragment of uracil. The barrier-free nature of the proton transfer process has been confirmed using the MPW1K functional as well as the MP2 method.

The anionic complexes with the O8 site protonated are the most stable. These complexes can be viewed as a neutral radical of hydrogenated uracil solvated by a deprotonated alanine. They are characterized by the largest values of VDE, which span a range of EBE=2.0–1.7 eV. These values of VDE were obtained by correcting the B3LYP values downward by 0.2 eV, as suggested by the CCSD(T) results for the valence anionic state of an isolated uracil molecule.

There are numerous structures of the neutral uracil–alanine complexes, which do not undergo a barrier-free proton transfer upon attachment of an excess electron. These are primarily structures with alanine coordinated to the O7 atom rather than to O8. Some of these structures are the most stable among the neutral complexes, but their favorable networks of hydrogen bonds cannot compensate for the unfavorable excess electron binding energies. The calculated vertical electron detachment energies for structures of this type are in a range of 0.9–1.7 eV and some of these structures may contribute to the broad photoelectron peak.

In view of the similarity between the photoelectron spectra of the anionic uracil–glycine and uracil–alanine complexes, we suggest that the same mechanism of barrier-free proton transfer might be operative in complexes of uracil with different amino acids. This mechanism involves the carboxylic group of an amino acid rather than a residual hydrophobic group. Important issues for future experimental and theoretical studies are: (i) what are propensities of thymine and cytosine to BFPT in complexes with amino acids, (ii) how do amino acids with hydrophilic side chains, such as aspartic or glutamic acids, interact with nucleic acid bases, and (iii) what are molecular species other than amino acids, which can also be involved in barrier-free proton transfer to nucleic acid bases.

Lastly, the formation of neutral radicals of hydrogenated pyrimidine bases may be relevant to DNA and RNA damage by low energy electrons. For instance, the neutral radical thymine-H[•], with the O8 atom protonated, cannot form a hydrogen bond with adenine, as dictated by the Watson–Crick pairing scheme. Such a radical might also react with an

adjacent deoxyribose molecule triggering strand-breaks in DNA.

ACKNOWLEDGMENTS

This work was supported by the (i) Polish State Committee for Scientific Research (KBN) Grant No. 4 T09A 012 24; (ii) US DOE Office of Biological and Environmental Research, Low Dose Radiation Research Program (M.G.); (iii) NSF Grant No. CHE-0211522 (K.B.). The calculations were performed at CYFRONET in Krakow (Grant No. KBN/SGI2800/UGdanski/051/2002 to I.D.) and at the National Energy Research Scientific Computing Center (NERSC). PNNL is operated by Battelle for the U.S. DOE under Contract No. DE-AC06-76RLO 1830. I.D. acknowledges the hospitality of Professor H.-H. Limbach at the Free University of Berlin.

- ¹B. Boudaïffa, P. Cloutier, D. Hunting, M. A. Huels, and L. Sanche, *Science* **287**, 1658 (2000).
- ²C. J. Burrows and J. G. Muller, *Chem. Rev.* **98**, 1109 (1998).
- ³B. Armitage, *Chem. Rev.* **98**, 1171 (1998).
- ⁴J. H. Miller, W. W. Wilson, and R. H. Ritchie, in *Computational Approaches in Molecular Radiation Biology*, edited by M. N. Varma and J. Chatterjee (Plenum, New York, 1994), pp. 65–76.
- ⁵L. Sanche, *Mass Spectrom. Rev.* **21**, 349 (2002).
- ⁶R. Barrios, P. Skurski, and J. Simons, *J. Phys. Chem. A* **106**, 7991 (2002).
- ⁷C. Desfrancois, S. Carles, and J. P. Schermann, *Chem. Rev. (Washington, D.C.)* **100**, 3943 (2000).
- ⁸S. Xu, J. M. Nilles, and K. H. Bowen, *J. Chem. Phys.* **119**, 10696 (2003).
- ⁹R. Weinkauff, J.-P. Schermann, and M. S. de Vries, *Eur. Phys. J. D* **20**, 309 (2002), and references therein.
- ¹⁰N. A. Oyler and L. Adamowicz, *J. Phys. Chem.* **97**, 11122 (1993).
- ¹¹O. Dolgounitcheva, V. G. Zakrzewski, and J. V. Ortiz, *Chem. Phys. Lett.* **307**, 220 (1999).
- ¹²O. Dolgounitcheva, V. G. Zakrzewski, and J. V. Ortiz, *J. Phys. Chem. A* **103**, 7912 (1999).
- ¹³M. Gutowski, P. Skurski, and J. Simons, *J. Am. Chem. Soc.* **122**, 10159 (2000).
- ¹⁴P. Skurski, J. Rak, J. Simons, and M. Gutowski, *J. Am. Chem. Soc.* **123**, 11073 (2001).
- ¹⁵S. S. Wesolowski, M. L. Leininger, P. N. Pentchev, and H. F. Schaefer III, *J. Am. Chem. Soc.* **123**, 4023 (2001).
- ¹⁶M. Gutowski, I. Dabkowska, J. Rak, S. Xu, J. M. Nilles, D. Radisic, and K. H. Bowen, Jr., *Eur. Phys. J. D* **20**, 431 (2002).
- ¹⁷X. F. Li, Z. L. Cai, and M. D. Sevilla, *J. Phys. Chem. A* **106**, 1596 (2002).
- ¹⁸M. D. Sevilla, B. Besler, and A. O. Colson, *J. Phys. Chem.* **99**, 1060 (1995).
- ¹⁹P. O. Lowdin, *Rev. Mod. Phys.* **35**, 724 (1963).
- ²⁰X. Li, Z. Cai, and M. D. Sevilla, *J. Phys. Chem. A* **105**, 10115 (2001).
- ²¹K. J. Kise and J. A. Shin, *Bioorg. Med. Chem.* **9**, 2485 (2001).
- ²²J. V. Coe, J. T. Snodgrass, C. B. Freidhoff, K. M. McHugh, and K. H. Bowen, *J. Chem. Phys.* **87**, 4302 (1987).
- ²³J. V. Coe, J. T. Snodgrass, C. B. Freidhoff, K. M. McHugh, and K. H. Bowen, *J. Chem. Phys.* **84**, 618 (1986).
- ²⁴I. Dabkowska, J. Rak, and M. Gutowski, *J. Phys. Chem. A* **106**, 7423 (2002).
- ²⁵A. D. Becke, *Phys. Rev. A* **38**, 3098 (1988).
- ²⁶A. D. Becke, *J. Chem. Phys.* **98**, 5648 (1993).
- ²⁷C. Lee, W. Yang, and R. G. Paar, *Phys. Rev. B* **37**, 785 (1988).
- ²⁸B. J. Lynch, P. L. Fast, M. Harris, and D. G. Truhlar, *J. Phys. Chem. A* **104**, 21 (2000).
- ²⁹R. Ditchfield, W. J. Hehre, and J. A. Pople, *J. Chem. Phys.* **54**, 724 (1971).
- ³⁰W. J. Hehre, R. Ditchfield, and J. A. Pople, *J. Chem. Phys.* **56**, 2257 (1972).
- ³¹T. van Mourik, S. L. Price, and D. C. Clary, *J. Phys. Chem. A* **103**, 1611 (1999).
- ³²J. C. Rienstra-Kiracofe, G. S. Tschumper, and H. F. Schaefer III, *Chem. Rev.* **102**, 231 (2002).
- ³³M. J. Frisch, G. W. Trucks, H. B. Schlegel *et al.*, GAUSSIAN 98, Gaussian, Inc., Pittsburgh, PA, 1998.
- ³⁴R. J. Harrison, J. A. Nichols, T. P. Straatsma *et al.*, NWCHEM, A Computational Chemistry Package for Parallel Computers, Version 4.0.1, Pacific Northwest National Laboratory, Richland, WA 99352-0999.
- ³⁵J. H. Hendricks, S. A. Lyapustina, H. L. de Clercq, and K. H. Bowen, *J. Chem. Phys.* **108**, 8 (1998).
- ³⁶I. Dabkowska and M. Gutowski (unpublished).
- ³⁷K. Afatooni, B. Hitt, G. A. Gallup, and P. D. Burrow, *J. Chem. Phys.* **115**, 6489 (2001).
- ³⁸T. P. Debies and J. W. Rabalais, *J. Electron. Spectrosc. Relat. Phenom.* **3**, 315 (1974).
- ³⁹A. Padva, P. R. LeBreton, R. J. Dinerstein, and J. N. A. Ridyard, *Biochem. Biophys. Res. Commun.* **60**, 1262 (1962).

The Journal of Chemical Physics is copyrighted by the American Institute of Physics (AIP). Redistribution of journal material is subject to the AIP online journal license and/or AIP copyright. For more information, see <http://ojps.aip.org/jcpo/jcpcr/jsp>
Copyright of Journal of Chemical Physics is the property of American Institute of Physics and its content may not be copied or emailed to multiple sites or posted to a listserv without the copyright holder's express written permission. However, users may print, download, or email articles for individual use.